

Aspects of ICRF-3

Chopo Ma¹, Daniel MacMillan², Karine Le Bail², David Gordon²

Abstract The Second Realization of the International Celestial Reference Frame (ICRF2) used dual-frequency VLBI data acquired for geodetic and astrometric purposes from 1979–2009 by organizations coordinated by the IVS and various precursor networks. Since 2009 the data set has been significantly broadened, especially by observations in the southern hemisphere. While the new southern data have ameliorated the north/south imbalance of observations, they appear to produce a systematic zonal declination change in the catalog positions. Over the 35 years of the ICRF data set the effect of galactic aberration may be significant. Geophysical and tropospheric models also may affect the source positions. All these effects need to be addressed in preparation for ICRF-3.

Keywords ICRF, observing program, declination, troposphere, galactic aberration

1 Data Distribution

ICRF2 was dominated by data from northern hemisphere stations. Figure 1 shows the evolution of the distribution of observations between northern and southern hemisphere stations from 1980 to 2015. As more southern hemisphere stations were added, the distribution has evolved from mainly northern to ~35% southern. Figure 2 shows the evolution of the observation distribution between northern hemisphere, south-

ern hemisphere, and mixed baselines. The distribution has evolved from mainly northern to ~20% mixed and ~20% southern.

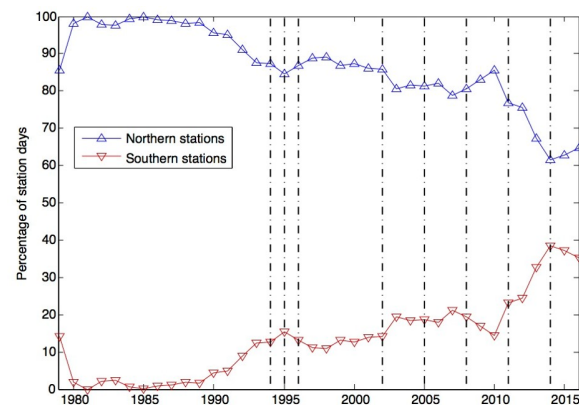


Fig. 1 Site observation distribution from 1980 to 2015 between northern sites (blue triangles) and southern hemisphere sites (red inverted triangles) as percentage of station days.

Figure 3 shows the growth of observations from 1980 to 2015. When ICRF2 was implemented in 2009, there were ~6.7 million observations from 4,726 sessions. Currently (as of 2016), there are ~10.7 million observations from 5,889 sessions. Southern hemisphere only and N-S baselines have increased noticeably in recent years but still represent only ~15% of the total.

Figure 4 shows the distribution of sources by number of sessions in the current (February 2016) solution. The largest group of sources (mostly VCS) has been observed in only two sessions. This however is a significant improvement over ICRF2, where ~2/3 of the sources (also mostly VCS) were observed only once.

1. NASA GSFC
2. NVI Inc./NASA GSFC

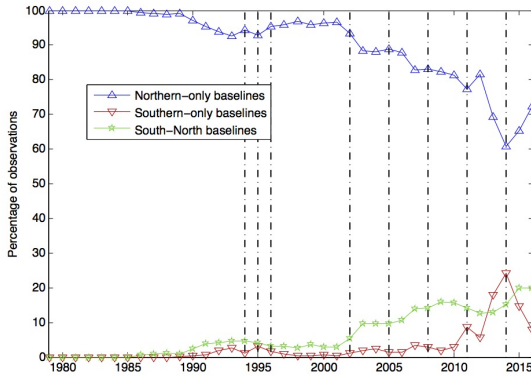


Fig. 2 Baseline observation distribution from 1980 to 2015 between baselines with only northern hemisphere stations (blue triangles), only southern hemisphere stations (red inverted triangles), and both northern and southern stations (green stars).

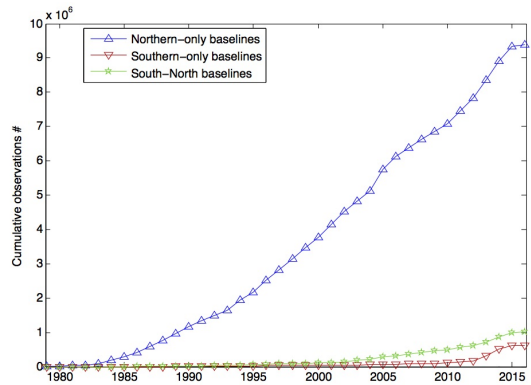


Fig. 3 Cumulative observations from 1980 to 2015. Currently there are ~ 9.16 million observations from purely northern hemisphere baselines (blue triangles), ~ 0.61 million from purely southern hemisphere baselines (red inverted triangles), and ~ 0.98 million from mixed baselines (green stars).

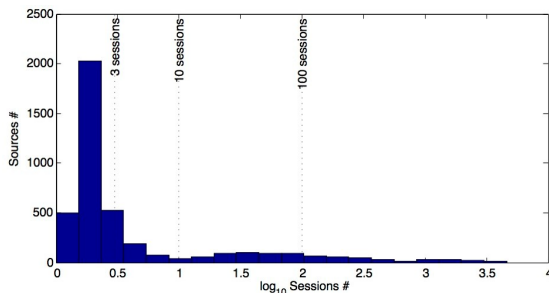


Fig. 4 Number of sources observed by session count in the current solution. Each histogram category shows the number of sources that were observed in a given number of sessions.

Recently it was found that 500 ICRF2 sources had not been reobserved since ICRF2. These sources are

predominantly weaker non-VCS sources, with 310 in the north and 190 in the south. An effort is underway to reobserve them; 65 have now been reobserved from a set of 100 sources added to the source monitoring program in October 2015. More of these sources will soon be added to the monitoring list.

2 Precision Improvement Since ICRF2

Figures 5a and b show the precision of the current (February 2016) solution, in μs . The distribution is much narrower than in ICRF2, with most sources better than $150 \mu\text{s}$ in right ascension (RA) and $250 \mu\text{s}$ in declination (DEC).

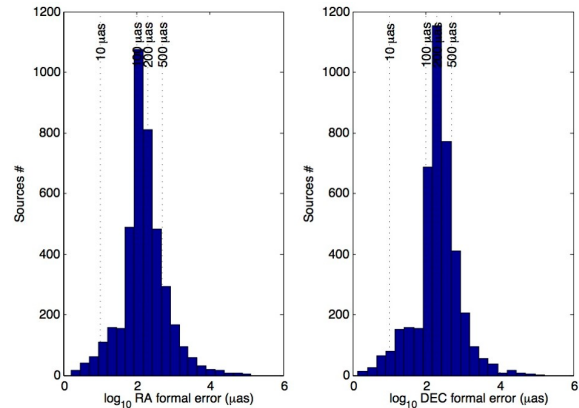


Fig. 5 Precision of sources in the current (February 2016) solution, in μs . Histograms show how many sources were observed at a given precision in right ascension (a) and declination (b).

Efforts have been made to improve the observations of the defining sources since ICRF2. Figures 6a and b compare the precision of the ICRF2 defining sources from the ICRF2 solution with the current solution. In ICRF2, 53 defining sources were observed in 18 or fewer sessions. By the end of 2015, all have been observed in at least 19 sessions due to the IVS VLBI source monitoring program.

Decimation tests were made to estimate the improvement of position uncertainties for non-VCS sources since ICRF2. Sessions were divided chronologically into two groups (even and odd sessions) and solutions were performed for each group for the ICRF2 data set and the current data set. The variance of the differences in source position estimates from the

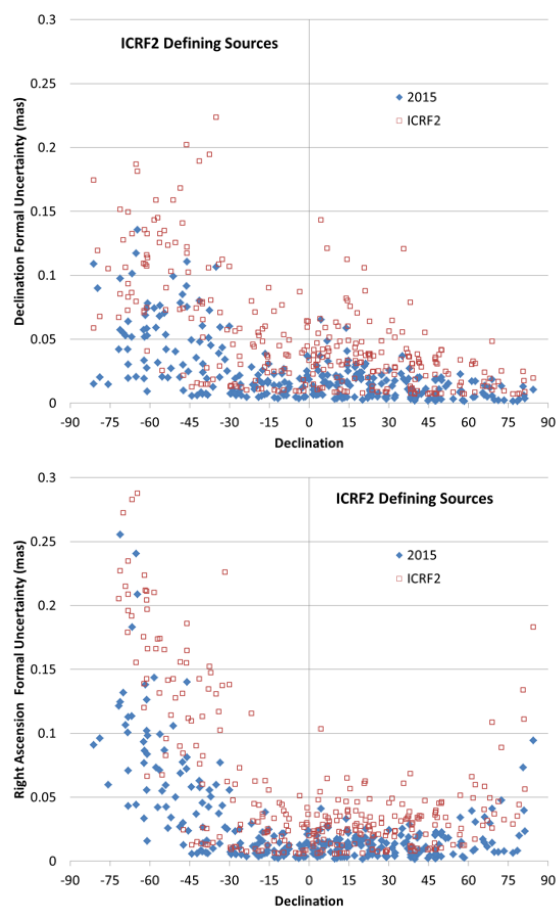


Fig. 6 Observations of ICRF2 defining sources in ICRF2 (open red squares) and after 2015 (filled blue diamonds). a) Declination formal uncertainty (mas) vs. declination. b) Right ascension formal uncertainty (mas) vs. declination.

two solutions gives an estimate of the average source position noise (uncertainty). For the ICRF2 data set we get RA and DEC. WRMS's of 52 and 62 μ as for 794 sources. For the current dataset, it decreases to 32 and 43 μ as for 883 sources.

Table 1 Average and median improvement in the precision of ICRF2–*Gaia* transfer sources. From Le Bail et al., 2016 [1].

Group	#	RA (mas)		DEC (mas)	
		2011b	2015a	2011b	2015a
1	89	0.017/0.011	0.011/0.007	0.017/0.013	0.011/0.008
2	66	0.032/0.020	0.022/0.015	0.032/0.027	0.021/0.018
3	16	0.052/0.053	0.033/0.033	0.080/0.064	0.037/0.033
4	24	0.869/0.251	0.128/0.066	1.903/0.345	0.163/0.092

Efforts have been made to improve the uncertainties of a set of 195 optically bright sources for use in aligning *Gaia* with ICRF-3. Table 1 shows the average and median precision improvement of these ICRF2–*Gaia* transfer sources since the start of this effort (RA uncertainties are not corrected for cosine DEC).

3 Systematic Effects

3.1 Zonal Declination

Figure 7 compares the positions of the defining sources from a recent solution with their ICRF2 positions. Each plot subtracts the ICRF2 positions from the current solution values for declination (a) and right ascension (b). The comparison reveals a zonal systematic in declination estimates with a peak of ~ 0.1 mas at $20\text{--}30^\circ$ S. This systematic is apparently caused by data from the four AUST stations that started observing in 2010. Figure 8 shows the resulting differences after excluding all data from the AUST network sessions as well as all AUST observations in other networks. The systematic is removed. Additional solutions have shown that removing either KATH12M or HOBART12 removes a significant part, but not all, of the zonal systematic. It is not clear from these tests whether there is a systematic error in ICRF2, a systematic instrumental effect from the AUST antennas, or a systematic effect due to the geometry of the AUST observing network.

3.2 Troposphere Delay Modeling

Figures 9a and b show the results of changing the elevation cutoff in (a) a 1980–2014 solution, and (b) the ICRF2 solution. Each solution was run with both a 15° cutoff and a 5° cutoff. The differences between the resulting declination estimates are plotted. The difference between the estimated parameters from the solutions is a measure of the troposphere model error, since the troposphere error at 15° is very small and it increases strongly as elevation decreases to 5° . The test shows that there is no clear systematic difference between the two cutoffs.

Three other tests were run. First, gradient constraints were weakened by a factor of 100. Next

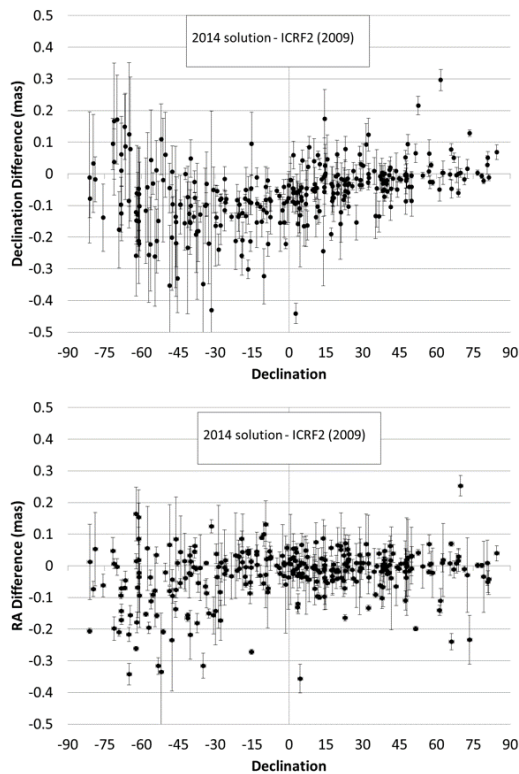


Fig. 7 Current CRF solution vs. ICRF2 solution: current values minus ICRF2 values. a) Declination differences and b) right ascension differences.

the results of elevation-dependent weighting were compared to results from using an elevation cutoff. Finally, a solution was run with ITRF2014 modeling of earthquakes instead of session-by-session estimation of post-seismic displacements. None of these tests produced a significant change in the systematic zonal declination effect.

3.3 Aberration

Figure 10a plots the proper motion due to the component of the galactic acceleration vector towards the Galactic center. MacMillan [2] estimated this component in a VLBI solution to be $5.3 \pm 0.3 \mu\text{as}/\text{year}$. For comparison, one can compute this acceleration from the radial distance to the Galactic center and the circular rotation speed of the solar system around the Galactic center, which can be determined from parallax mea-

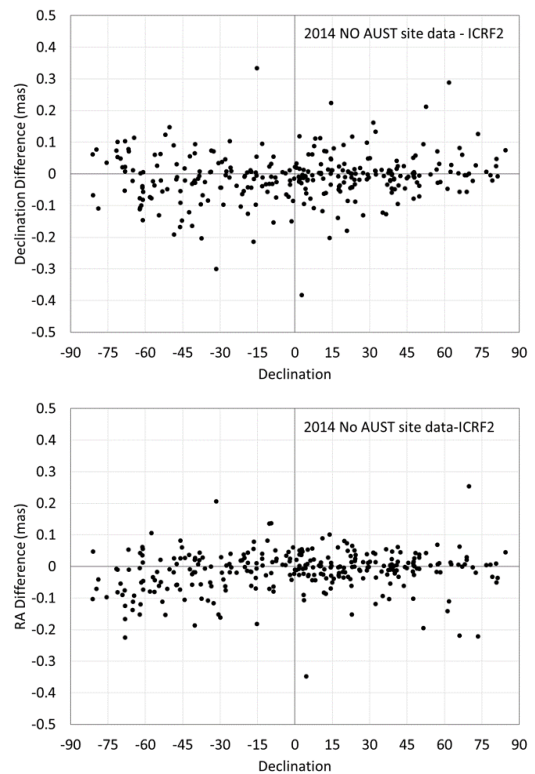


Fig. 8 Effect of removing the AUST stations from the current solution: current values (without AUST) minus ICRF2 values. a) Declination differences and b) right ascension differences.

surements. Using the values from Reid et al. [3] leads to an aberration vector magnitude of $4.9 \pm 0.4 \mu\text{as}/\text{year}$.

For contrast, Figure 10b plots the raw proper motion field computed from a source position time series for sources with right ascension and declination proper motion uncertainties less than $50 \mu\text{as}$ per year. The plot shows that the aberration effect is much smaller than the random apparent motions, which are likely due to source structure.

4 Conclusions

The cumulative number of observations when ICRF2 was generated in 2009 was 6.7 million. This number has increased to 10.7 million observations in the present solution. The strongest 100 sources from the 500 sources not reobserved since ICRF2 are now being reobserved. At least 65 have been observed since Oc-

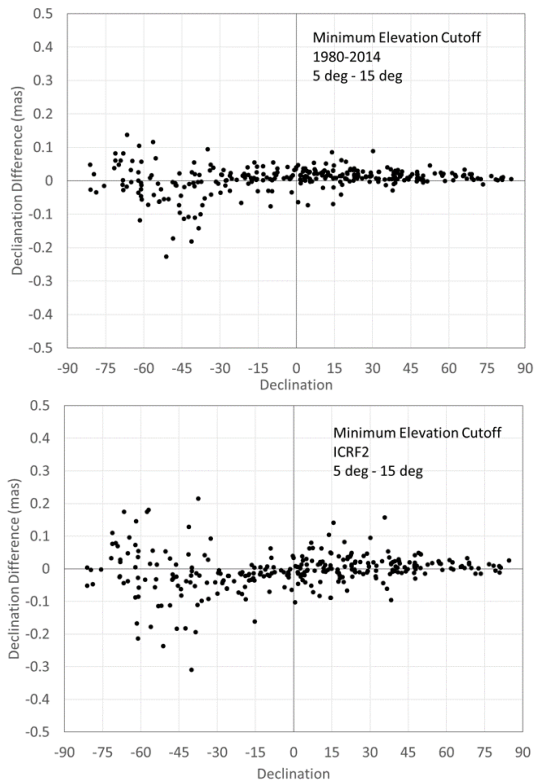


Fig. 9 Declination estimates from a solution with a 5° minimum elevation cutoff minus declination estimates from a solution with a 15° cutoff. a) 2014 solution and b) the ICRF2 solution.

tober 2015. The average source position uncertainty of the non-VCS sources has improved since ICRF2. The most recent solution has decreased the average right ascension uncertainty from $52 \mu\text{s}$ to $32 \mu\text{s}$ and the average declination uncertainty from $62 \mu\text{s}$ to $43 \mu\text{s}$. The ICRF2–*Gaia* transfer source precision has also improved significantly since 2011. The precision for 295 ICRF2 defining sources has improved for all declinations. Comparing declinations from a current CRF solution to declinations from the ICRF2 solution reveals a systematic zonal dependence, with a maximum of ~ 0.1 mas at $20\text{--}30^\circ\text{S}$. Tests of troposphere modeling do not appear to explain this. But removing data from four AUST stations removes the systematic. It is unclear whether there is a systematic error in ICRF2 or a systematic instrumental effect due to the AUST antennas or a systematic effect due to the geometry of AUST observing.

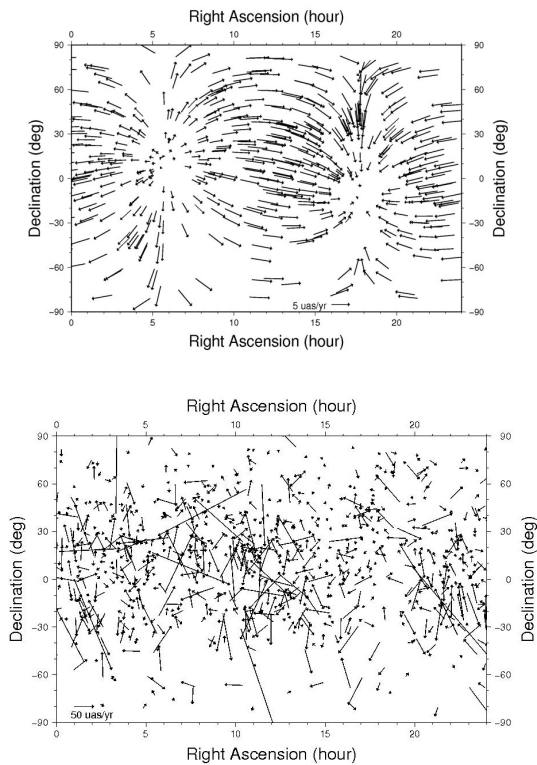


Fig. 10 a) Proper motion due to the component of acceleration vector towards the Galactic center. b) Raw proper motion field for sources with uncertainties better than $50 \mu\text{as/yr}$.

References

1. K. Le Bail, J. M. Gipson, D. Gordon, D. S. MacMillan, D. Behrend, C. C. Thomas, S. Bolotin, W. E. Himwich, K. D. Baver, B. E. Corey, M. Titus, G. Bourda, P. Charlot, and A. Collioud, “IVS Observation of ICRF2–*Gaia* Transfer Sources”, In *The Astronomical Journal*, 151:79, 2016, doi:10.3847/004-6256/151/3/79.
2. D. S. MacMillan, “Determination of Galactic Aberration from VLBI Measurements and Its Effect on VLBI Reference Frames and Earth Orientation Parameters”, American Geophysical Union Meeting, Fall 2014.
3. M. J. Reid, K. M. Menten, A. Brunthaler, X. W. Zheng, T. M. Dame, Y. Xu, Y. Wu, B. Zhang, A. Sanna, M. Sato, K. Hachisuka, Y. K. Choi, K. Immer, L. Moscadelli, K. L. J. Rygl, and A. Bartkiewicz, “Trigonometric Parallaxes of High Mass Star Forming Regions: The Structure and Kinematics of the Milky Way”, *Astrophysical Journal*, vol. 783, Num. 2, p. 130, 2014.